Supplemental Figure 1

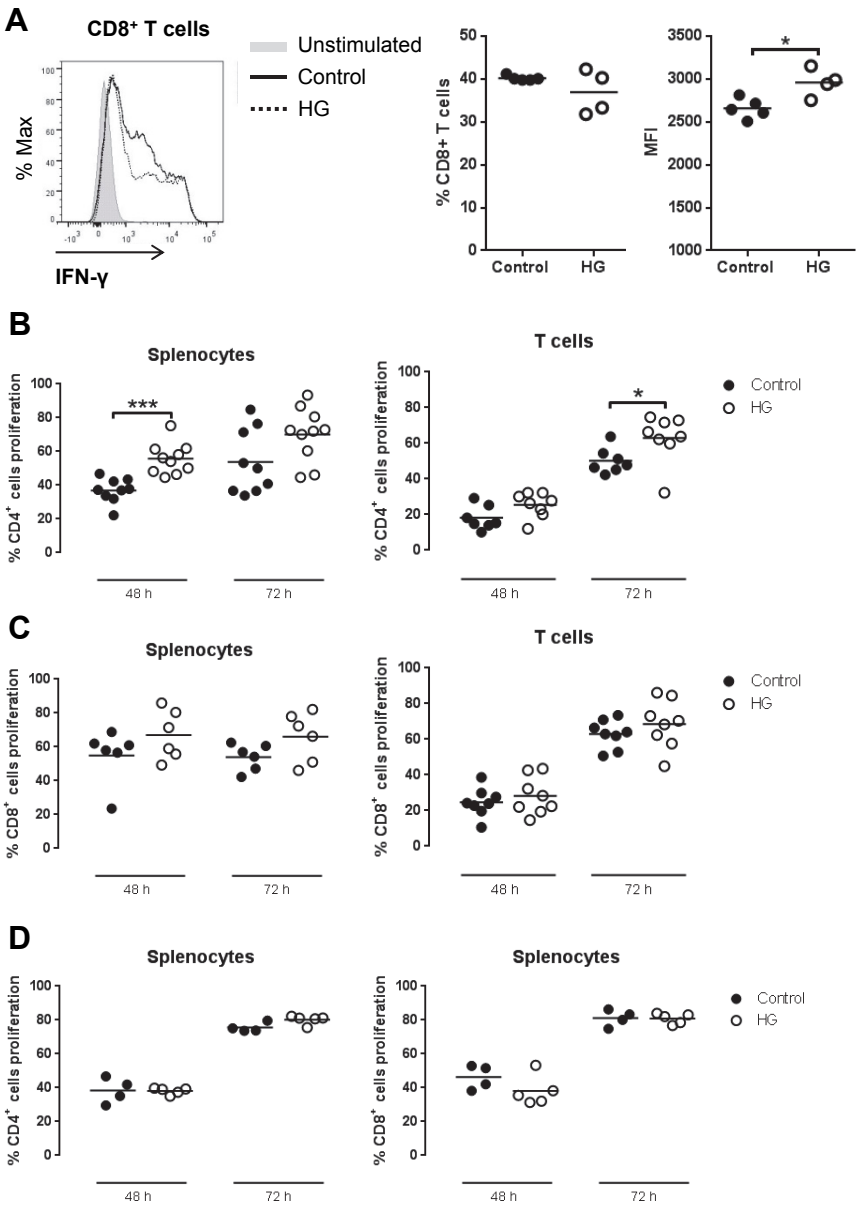

Supplemental Figure 1. IFN-γ production by anti-CD3 stimulated CD8$^+$ T cells and i*n vitro* CD4$^+$ and CD8$^+$ T cell proliferation in control and HG mice. A, Splenocytes were stimulated with plate-bound anti-CD3e (2.5 µg/ml) *in vitro* for 48 h and IFN-γ$^+$ cells were measured by intracellular staining. **B,** Splenocytes or isolated T cells (negative selection by magnetic beads, >95% T cells) from spleen and lymph nodes in control or HG mice were stimulated with plate-bound anti-CD3e (2.5 µg/ml) *in vitro* for 48 and 72 h. Proliferation of CD4$^+$ T cells in splenocytes (left graph, n=9-10) and in T cells (right graph, n=6-8) was detected by flow cytometry and CFSE dilution. **C,** Proliferation of CD8$^+$ T cells in splenocytes (left graph, n=6) and in T cells (right graph, n=8) was detected by flow cytometry and CFSE dilution. **D,** Proliferation of CD4$^+$ (left graph) and CD8$^+$ (right graph) T cells was detected in splenocytes from acute HG mice (≤4 wk) by flow cytometry and CFSE dilution (n=4-5). All experiments were repeated at least twice. Statistical differences were analyzed by Student's t test for each time point, *p<0.05.

Supplemental Figure 2

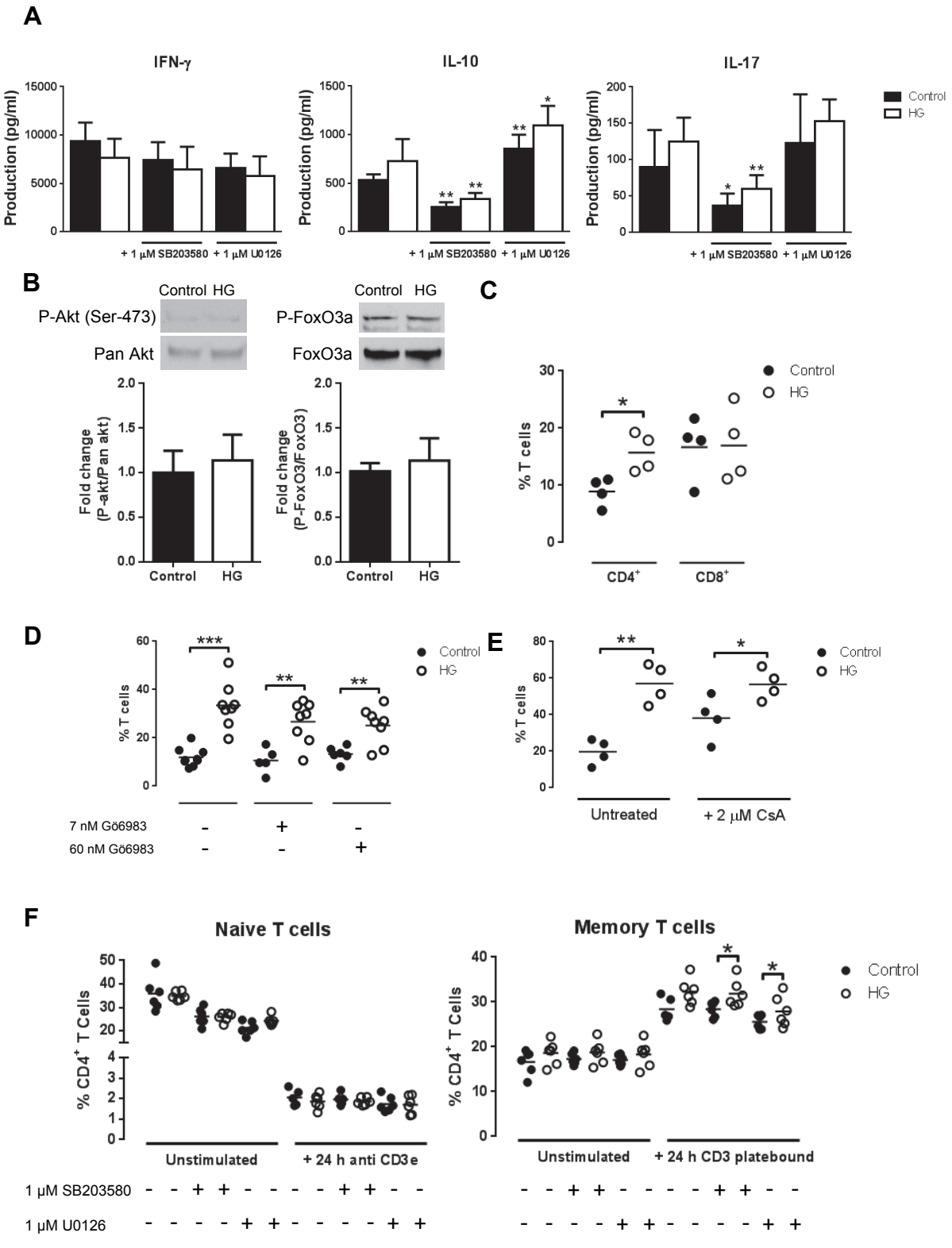

Supplemental Figure 2. Akt signaling and chromatin decondensation in T cells. Roles for PKC and calcineurin in chromatin decondensation and MAPK signaling in cytokine production and CD44 expression. A, Akt and FoxO3 phosphorylation in isolated T cells from control and HG mice (n=4-5). **B,** $CD4^+$ and $CD8^+$ T cells were isolated from control and HG mice by magnetic beads. Percentage of T cells with nuclei >6 μm in diameter (n=4). **C,** Percentage of T cells with nuclei >6 μm in diameter following treatment with the PKC inhibitor GO6983 at 7 or 60 nM that inhibit subunits α and β or ζ, respectively, for 5 h (n=5-8). **D,** Percentage of T cells with nuclei >6 μm in diameter following treatment with 2 μM cyclosporine A for 5 h (n=4). **E,** IFN-γ, IL-10 and IL-17 production in splenocytes from control or HG mice stimulated with plate-bound anti-CD3e and treated or not with 1 μM SB203580 (p38 inhibitor) or 1 μM U0126 (ERK inhibitor). **F,** Percentage of naïve T cells, $CD44^-CD62L^{high}$, or memory T cells, $CD44^+$, from control or HG mice unstimulated or stimulated with plate-bound anti-CD3e for 24 h and treated or not with 1 μM SB203580 (p38 inhibitor) or 1 μM U0126 (ERK1/2 inhibitor) (n=5). All experiments were repeated at least three times. Statistical differences were analyzed by Student's t test for each condition, *$p<0.05$, **$p<0.01$, ***$p<0.001$.

Supplemental Figure 3

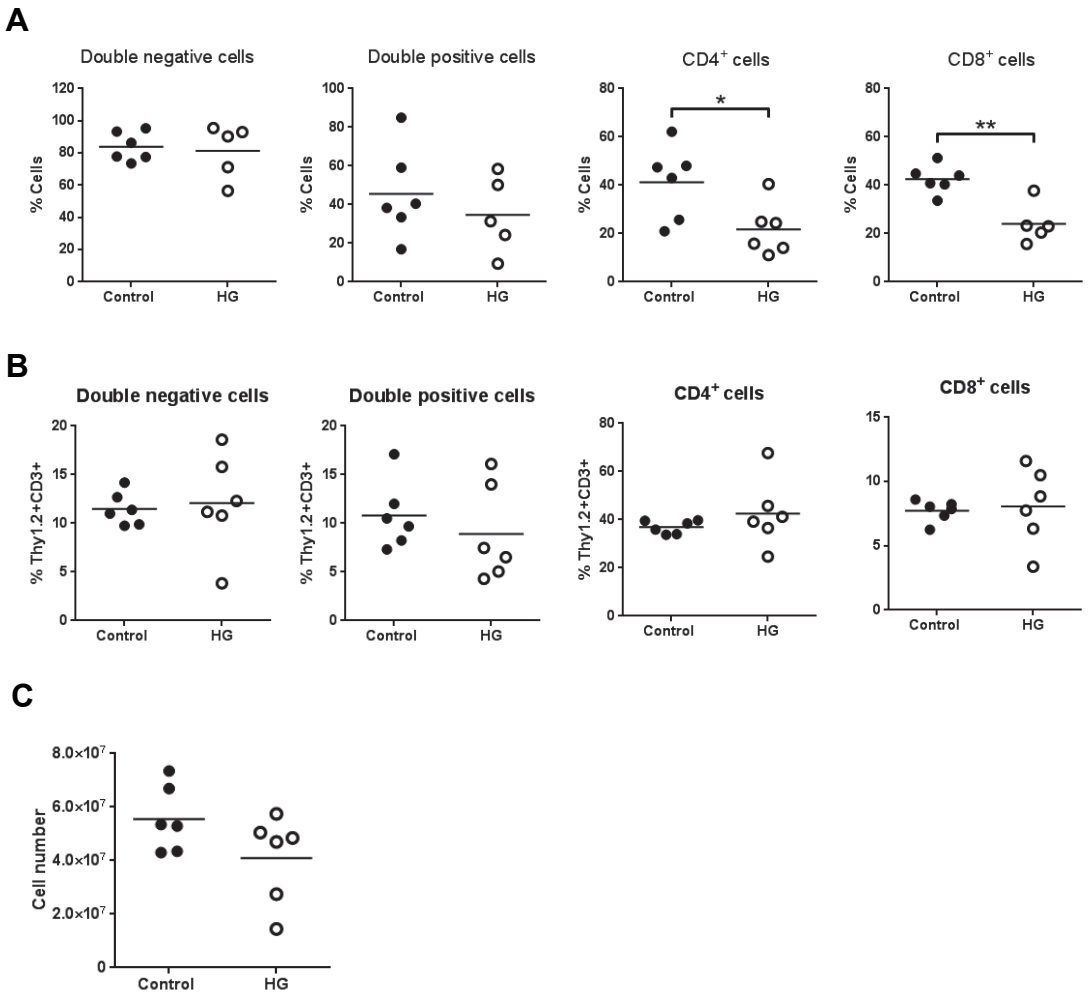

Supplemental Figure 3. Chromatin decondensation in thymocytes and thymocyte populations and total numbers in control and HG mice. Each population of thymocytes was sorted, cytospined and DAPI stained. Percentage of thymocytes with nuclei >6.5 µm in diameter. **A,** double-negative thymocytes, double-positive thymocytes, $CD4^+$ thymocytes, $CD8^+$ thymocytes (n=5). **B,** Thymocytes isolated from control and HG mice were counted and stained for Thy1.2, CD3, CD4 and CD8. Percentage of double-negative cells ($CD4^-CD8^-$), double-positive cells ($CD4^+CD8^+$) and single-positive cells (n=5). **C,** total thymocytes number (n=5). All experiments were repeated at least twice. Statistical differences were analyzed by Student's t test.

Supplementary Figure 4

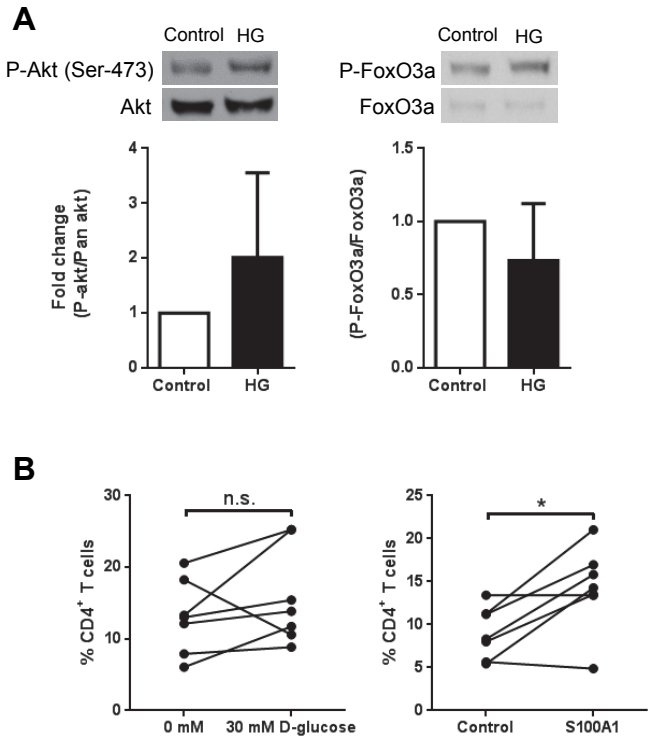

Supplemental Figure 4. Akt signaling in RAGE$^{-/-}$ mice and role of glucose and S100A1 roles in the nucleus decondensation *in vitro*. A, Basal Akt and FOXO3 phosphorylation was measured in isolated T cells from control and HG mice RAGE$^{-/-}$ mice (n=4). **B,** Isolated CD4+ T cells were treated with 30 mM D-glucose or 100 ng/ml S100A1 for 5 h and nuclei size was measured. Percentage of T cells with nuclei >6 μm in diameter (n=6). Statistical differences were analyzed by Student's t test, *p<0.05.